Cell Reports, Volume *35*

Supplemental information

Chronic stress physically spares but functionally impairs innate-like invariant T cells

Patrick T. Rudak, Joshua Choi, Katie M. Parkins, Kelly L. Summers, Dwayne N. Jackson, Paula J. Foster, Anton I. Skaro, Ken Leslie, Vivian C. McAlister, Vijay K. Kuchroo, Wataru Inoue, Olivier Lantz, and S.M. Mansour Haeryfar

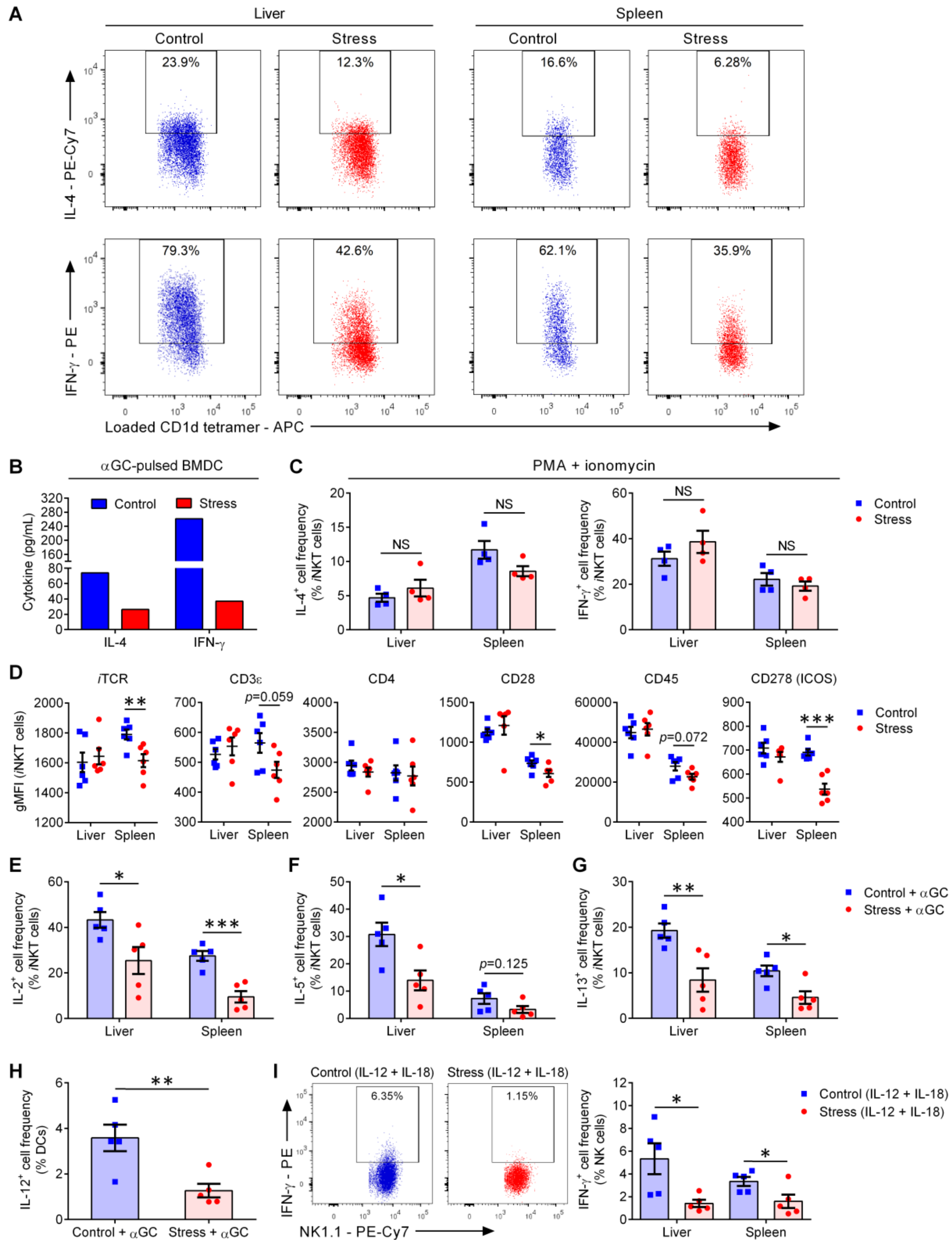

Supplemental Figure 1. Prolonged physical restraint impairs the ability of *i*NKT cells to elicit T$_H$1 and/or T$_H$2-type cytokine responses to αGC or to a combination of IL-12 and IL-18, but not to a combination of PMA

and ionomycin (related to Figure 1). (A) B6 mice were physically restrained (or not) for 12 h before they were given αGC. Two hours later, HMNCs and splenocytes were stained with mAbs against IL-4 and IFN-γ and analyzed by flow cytometry. Representative dot plots illustrate the frequencies of IL-4^{+} and IFN-γ^{+} *i*NKT cells after gates were set based on isotype control staining. **(B)** Sorted hepatic *i*NKT cells pooled from ≥5 stressed or control B6 mice were stimulated *ex vivo* with 100 ng/mL of αGC in the presence of CD11c^{+} BMDCs. After 24 h, IL-4 and IFN-γ levels in culture supernatants were measured. **(C)** HMNCs and splenocytes from stressed and control B6 mice were stimulated for 2 h with 15 ng/mL of PMA and 500 ng/mL of ionomycin before intracellular levels of IL-4 and IFN-γ in *i*NKT cells were determined by flow cytometry. **(D)** HMNCs and splenocytes from restrained or control animals were stained with loaded CD1d tetramer or mAbs against indicated molecules. After gating on *i*NKT cells, the gMFI of staining for each molecule is depicted. **(E-G)** As in (**A**), but summary data indicates the frequencies of *i*NKT cells staining positively for mAbs against IL-2 **(E)**, IL-5 **(F)** and IL-13 **(G)**. **(H)** B6 mice were restrained (or not) for 12 h before they were given αGC. Six h later, HMNCs were stained with an anti-IL-12p35 mAb or a rat IgG2aκ isotype control. The frequency of IL-12^{+} DCs was determined after gating on TCRβ^{-}CD11c^{+} events. **(I)** Mice that had been restrained or left undisturbed were injected with IL-12 and IL-18 one h before the percentages of IFN-γ^{+} events among TCRβ^{-}NK1.1^{+} NK cells were determined. Representative flow plots and summary data are shown. Each symbol represents an individual mouse, and error bars represent SEM. *, ** and *** denote significant differences with p<0.05, p<0.01 and p<0.001, respectively, by unpaired Student's *t*-tests. NS = not significant

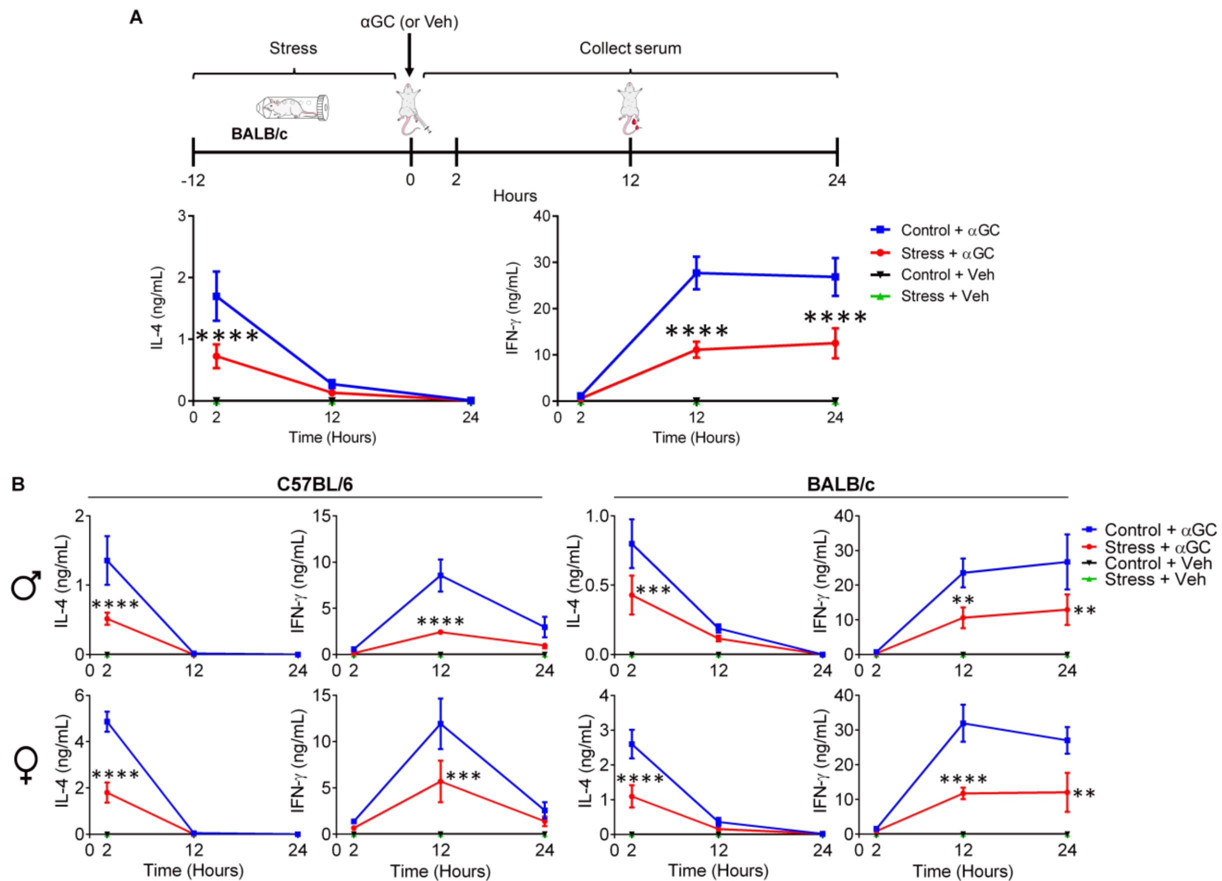

Supplemental Figure 2. Prolonged stress impairs cognate *i*NKT cell responses in male and female B6 and BALB/c mice (related to Figure 1). (A) WT BALB/c mice were subjected to physical restraint or left undisturbed for 12 h before they were injected i.p. with αGC or Veh. At indicated time points, IL-4 and IFN-γ in serum samples were quantified by ELISA (n=8-9/group). **(B)** Data presented in Figure 1B-C and Figure S2A were segregated by sex. The kinetics of serum cytokine levels following αGC (or Veh) administration in male (B6: n=5; BALB/c: n=5) and female (B6: n=5; BALB/c: n=3-4) mice are depicted. Error bars represent SEM. **, *** and **** denote differences with $p<0.01$, $p<0.001$ and $p<0.0001$, respectively, using two-way ANOVA with Dunnett's post-hoc analysis.

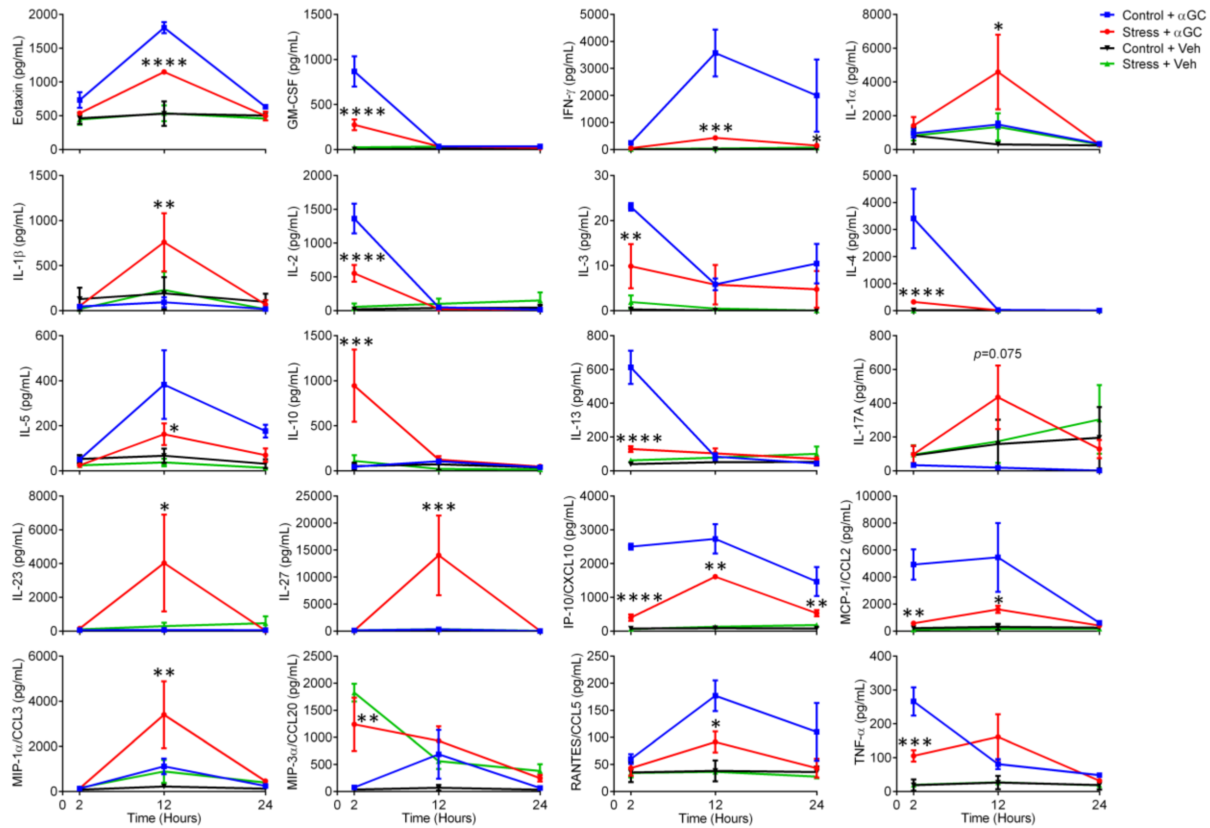

Supplemental Figure 3. Prolonged physical restraint before αGC administration alters the serum concentrations of a wide range of inflammatory mediators (related to Figure 1). WT B6 mice were restrained or left undisturbed for 12 h before they were injected with αGC or Veh (n=3/cohort). Two, 12 and 24 h later, mice were bled and serum levels of indicated mediators were quantified by cytokine/chemokine multiplexing. *, **, *** and **** denote significant differences between stressed and control animals receiving αGC with $p<0.05$, $p<0.01$, $p<0.001$ and $p<0.0001$, respectively, using two-way ANOVA with Tukey's post-hoc analysis.

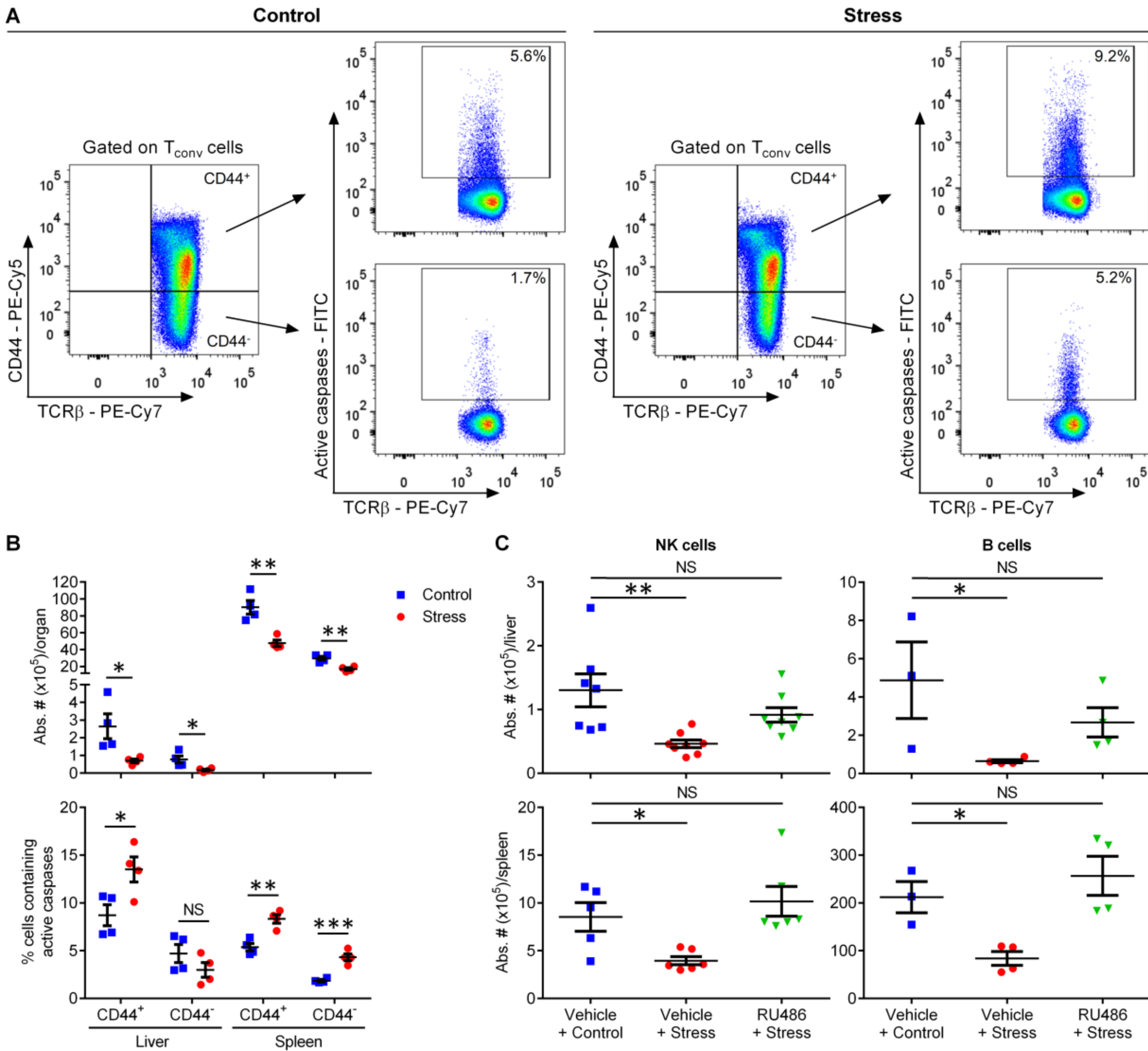

Supplemental Figure 4. Unlike *i*NKT cells, naïve and memory T_{conv} cells, NK cells and B cells are prone to stress-induced apoptosis (related to Figure 2). (A-B) Splenocytes and HMNCs from restrained and control B6 mice were stained for surface TCRβ, surface CD44 and intracellular active caspases. A rat IgG2bκ isotype control was used to set the gate for CD44 staining. **(A)** Representative FACS plots illustrate our gating strategy to distinguish between splenic $CD44^+$ and $CD44^-$ populations among $TCR\beta^+CD1d$ $tetramer^-$ events, which correspond to memory and naïve T_{conv} cells, respectively. Gates containing T_{conv} cells with intracellular active caspases are also shown. **(B)** The absolute numbers of hepatic and splenic memory and naïve T_{conv} cells and the percentages of T_{conv} cells staining positively for active caspases are depicted. **(C)** Separate cohorts of B6 mice were treated i.p. with RU486 or Veh.

One hour later, animals were subjected to prolonged restraint stress or were left undisturbed for 12 h. HMNCs and splenocytes were prepared shortly afterwards and stained with a panel of mAbs against TCRβ, NK1.1 and B220. $TCR\beta^{-}NK1.1^{+}$ NK cells and $TCR\beta^{-}B220^{+}$ B cells were identified by flow cytometry, and their absolute numbers were calculated. Each symbol represents an individual mouse, and error bars represent SEM. *, ** and *** denote differences with $p<0.05$, $p<0.01$ and $p<0.001$, respectively, using unpaired Student's *t*-tests (**B**) or one-way ANOVA with Dunnett's post-hoc analysis (**C**). NS = not significant

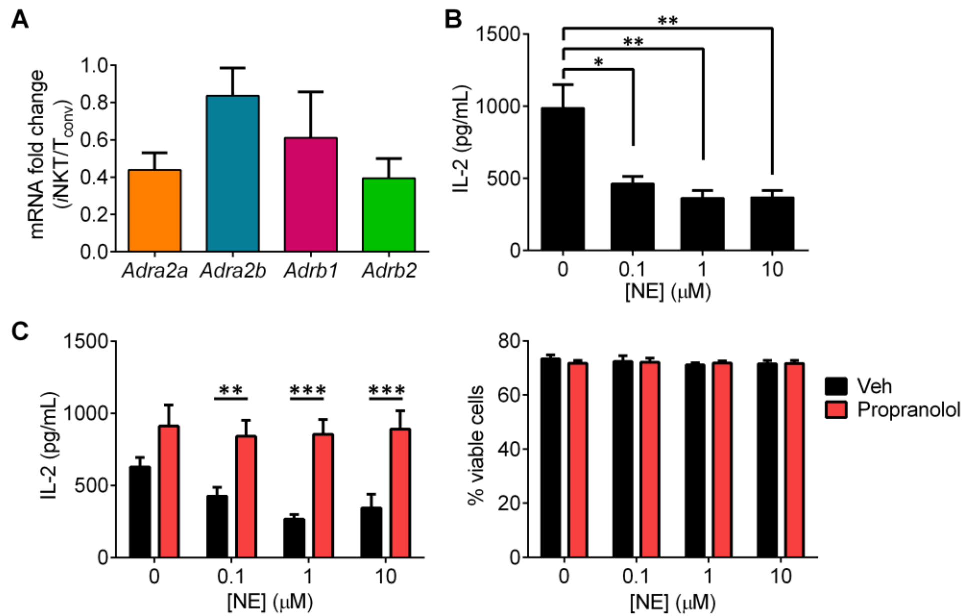

Supplemental Figure 5. *i*NKT cells express adrenergic receptors and respond weakly to αGC in the presence of NE in an *in vitro* setting (related to Figure 3). (A) HMNCs from 10 naïve B6 mice were pooled and co-stained with an anti-TCRβ mAb and PBS-57-loaded CD1d tetramers. *i*NKT and T_{conv} cells were FACS-purified for cDNA synthesis and gene expression analysis by quantitative PCR. The expression of indicated genes by *i*NKT cells relative to T_{conv} cells was calculated using the $2^{-(\Delta\Delta Ct)}$ method. Data from 3 independent experiments were used to determine fold change values. **(B)** DN32.D3 cells were exposed for 20 minutes to indicated concentrations of norepinephrine (NE) before they were stimulated with 100 ng/mL of αGC. The IL-2 content of culture supernatants was quantified after 24 h by ELISA (n=3-5). **(C)** DN32.D3 cells were pretreated for 20 minutes with propranolol before they were exposed to NE and subsequently stimulated with αGC (n=4). After 24 h, IL-2 was measured in supernatants (n=4) and cellular viability was assessed by 7-AAD staining (n=3). Error bars represent SEM. *, ** and *** denote differences with $p<0.05$, $p<0.01$ and $p<0.001$, respectively, by one-way ANOVA with Dunnett's post-hoc analysis (**B**) or by unpaired Student's *t*-tests (**C**).

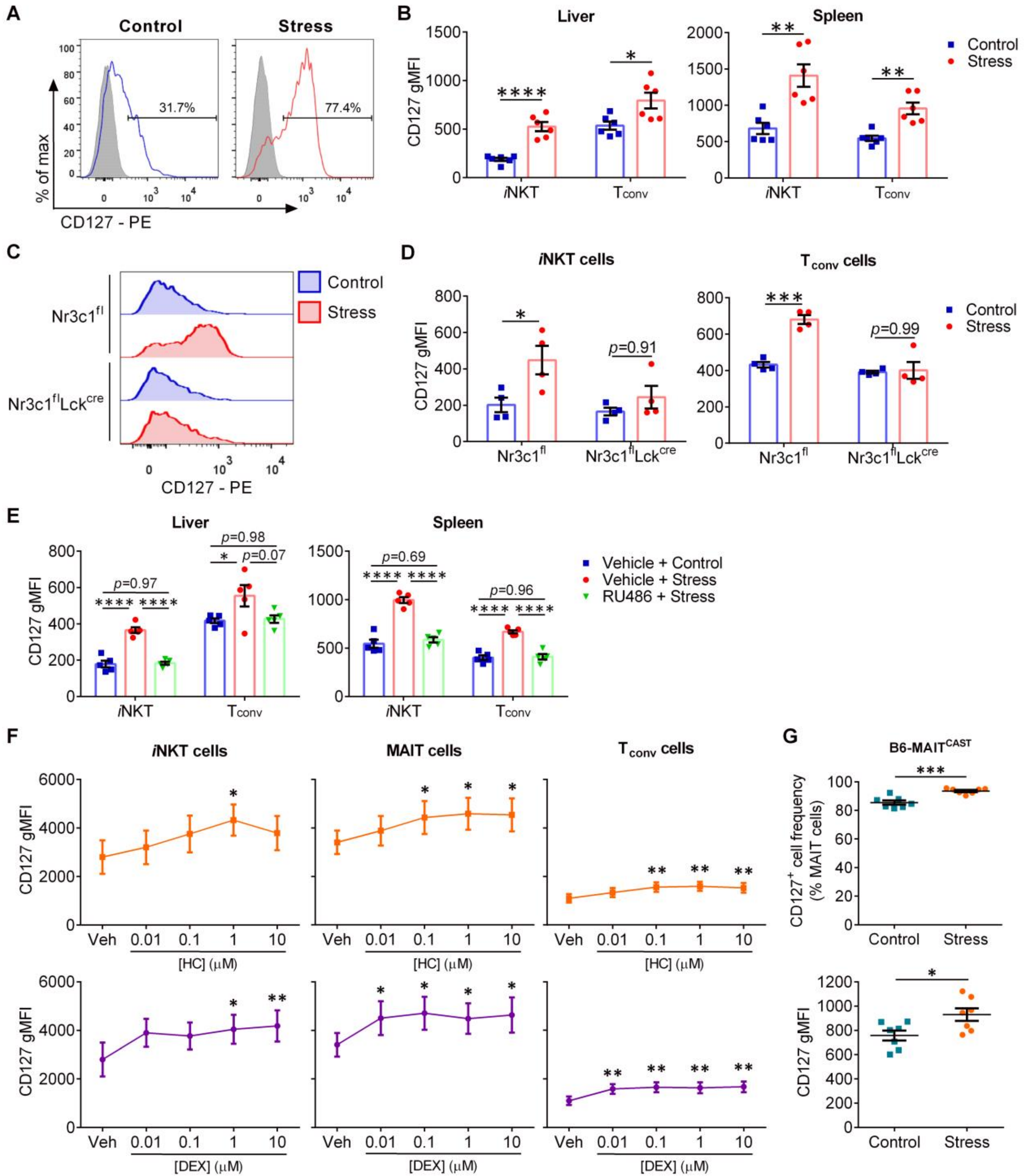

Supplemental Figure 6. Mouse and human *i*NKT, MAIT and T_{conv} cells upregulate CD127 in response to GR signaling (related to Figure 7). B6 mice were subjected to 12 h of restraint stress (or not). Shortly afterwards, HMNCs and splenocytes were prepared and stained to detect CD127 expression on the surface of *i*NKT and T_{conv}

cells. Open and filled histograms correspond to staining with an anti-CD127 mAb and a rat IgG2aκ isotype control, respectively, after gating on hepatic *i*NKT cells **(A)**. Cumulative data depicting the gMFI of CD127 staining in indicated populations are also shown **(B)**. $Nr3c1^{fl}$ and $Nr3c1^{fl}Lck^{cre}$ mice were physically restrained (or not) and assessed for CD127 expression in their *i*NKT and T_{conv} cell compartments **(C-D)**. Blue and red histograms correspond to CD127 expression on hepatic *i*NKT cells from control and stressed mice, respectively **(C)**, and cumulative data for indicated cell populations are summarized using bar graphs **(D)**. Separate cohorts of WT B6 mice received RU486 (or Veh) i.p. 1 h before they were physically restrained (or not). The gMFI of CD127 staining is shown **(E)**. Human PBMCs were cultured for 24 h in the presence of hydrocortisone (HC), dexamethasone (DEX) or vehicle before they were stained with either an anti-CD127 mAb or a mouse IgG1κ isotype control. The gMFI of CD127 staining in *i*NKT, MAIT and T_{conv} cells was assessed by flow cytometry (n=5) **(F)**. B6-$MAIT^{CAST}$ mice were physically restrained or left undisturbed for 12 h before they were sacrificed for their liver. HMNCs were stained with a mAb to CD127 or a rat IgG2aκ isotype control. After gating on $TCR\beta^{+}B220^{-}MR1$ $tetramer^{+}$ MAIT cells, the percentages of $CD127^{+}$ cells and the gMFI of CD127 staining were determined **(G)**. Each symbol in (**B**, **D-E** and **G**) represents an individual mouse. Error bars represent SEM. *, **, *** and **** denote differences with $p<0.05$, $p<0.01$, $p<0.001$ and $p<0.0001$, respectively, using unpaired Student's *t*-tests (**B**, **D** and **G**) or one-way ANOVA (**E-F**).

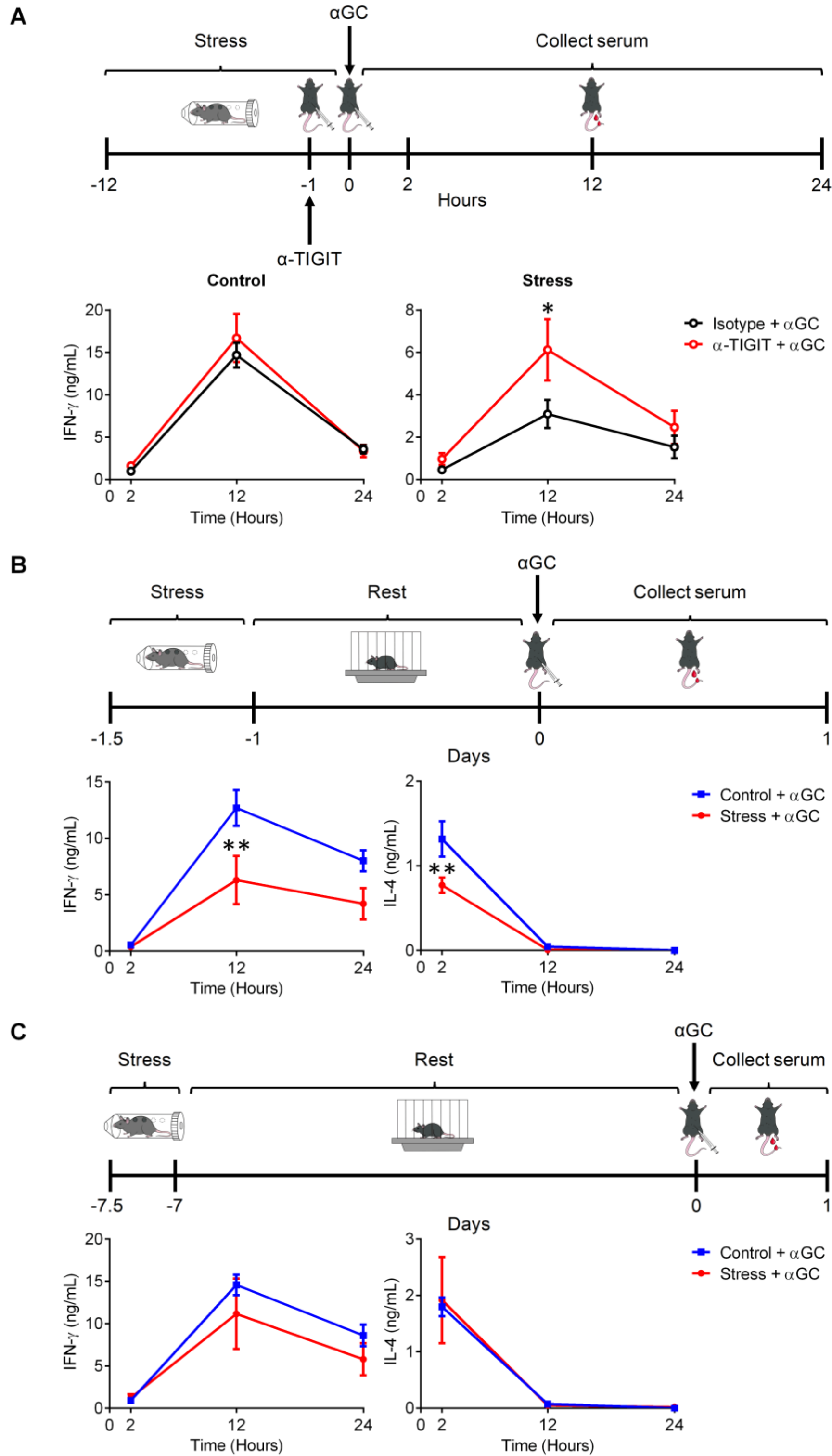

Supplemental Figure 7. Stress-induced *i*NKT cell impairments are partially mediated by TIGIT and do not last long after the stressor is removed (related to Figure 4). (A) B6 mice were restrained or left undisturbed

before they received a 200-µg i.p. dose of an anti-mouse TIGIT mAb (or a mouse IgG1κ isotype control) followed by αGC administration as schematically illustrated. Mice were bled at indicated time points, and serum IFN-γ levels were quantified (n=8-9/group). **(B-C)** Separate cohorts of B6 mice were physically restrained or left undisturbed for 12 h. Mice were then returned to standard housing conditions for one day **(B)** or seven days **(C)** before they were injected i.p. with αGC. Serum IFN-γ and IL-4 levels were measured at indicated time points (n=4/group). Error bars represent SEM. * and ** denotes differences with $p<0.05$ and $p<0.01$, respectively, using two-way ANOVA with Sidak's post-hoc analysis.

Supplemental Table 1: Taqman-based qPCR primer/probe sets used in this study (related to STAR Methods).

Target	Assay Identification
Abl1	Mm00802029_m1
Actb	Mm00607939_s1
Adra1a	Mm00442668_m1
Adra1b	Mm00431685_m1
Adra1d	Mm01328600_m1
Adra2a	Mm00845383_s1
Adra2b	Mm00477390_s1
Adra2c	Mm00431686_s1
Adrb1	Mm00431701_s1
Adrb2	Mm02524224_s1
Adrb3	Mm02601819_g1
Aifm1	Mm00442540_m1
Anxa5	Mm01293059_m1
Apaf1	Mm01223702_m1
Api5	Mm00500189_m1
Atf5	Mm04179654_m1
Bad	Mm00432042_m1
Bag1	Mm01208593_m1
Bag3	Mm00443474_m1
Bak1	Mm00432045_m1
Bax	Mm00432051_m1
Bbc3	Mm00519268_m1
Bcl2	Mm00477631_m1
Bcl2a1a	Mm03646861_mH
Bcl2l1	Mm00437783_m1
Bcl2l11	Mm00437796_m1
Bid	Mm00432073_m1
Bik	Mm00476123_m1
Birc2	Mm00431811_m1
Birc3	Mm01168413_m1
Birc5	Mm00599749_m1
Bmf	Mm00506773_m1
Bnip2	Mm00443990_m1
Card10	Mm00459941_m1
Card6	Mm01297056_m1
Casp1	Mm00438023_m1
Casp2	Mm00432314_m1
Casp3	Mm01195085_m1
Casp4	Mm00432307_m1
Casp6	Mm00438053_m1
Casp7	Mm00432324_m1
Casp8	Mm00802247_m1
Casp9	Mm00516563_m1
Cblb	Mm01343092_m1

Cd27	Mm01185212_g1
Cd28	Mm00483137_m1
Cd40lg	Mm00441911_m1
Cd44	Mm01277161_m1
Cd69	Mm01183378_m1
Cd274	Mm03048248_m1
Cdk2	Mm00443947_m1
Cdk4	Mm00726334_s1
Cflar	Mm01255578_m1
Cradd	Mm01226172_m1
Csf1	Mm00432686_m1
Dad1	Mm01319221_m1
Dffa	Mm00438410_m1
Dffb	Mm00432822_m1
Diablo	Mm01194441_m1
Egr2	Mm00456650_m1
Egr3	Mm00516979_m1
Fadd	Mm00438861_m1
Fas	Mm01204974_m1 Mm00433237_m1
Fasl	Mm00438864_m1
Fos	Mm00487425_m1
Foxo3	Mm01185722_m1
Foxp1	Mm00474848_m1
Gata3	Mm00484683_m1
Gzma	Mm01304452_m1
Gzmb	Mm00442834_m1
Hells	Mm00468580_m1
Icam1	Mm00516023_m1
Icos	Mm00497600_m1
Ifng	Mm01168134_m1
Ifnar1	Mm00439544_m1
Ifnar2	Mm00494916_m1
Igf1r	Mm00802831_m1
Il10ra	Mm00434151_m1
Il12rb1	Mm00434189_m1
Il18rap	Mm00516053_m1
Il2	Mm00434256_m1
Il2ra	Mm01340213_m1
Il2rb	Mm00434268_m1
Il4	Mm00445259_m1
Il7ra/Cd127	Mm00434295_m1
Irf4	Mm00516431_m1
Itch	Mm01246513_m1
Jak1	Mm00600614_m1
Jak3	Mm00439962_m1
Jun	Mm00495062_s1

Lat	Mm00456761_m1
Lta	Mm00440228_gH
Myb	Mm00501741_m1
Naip2	Mm00440446_m1
Nfatc1	Mm00479445_m1
Nfatc2	Mm00477776_m1
Nfatc3	Mm01249200_m1
Nfkb1	Mm00476361_m1
Notch1	Mm00435249_m1
Npy1r	Mm04208490_m1
Npy2r	Mm01218209_m1
Npy4r	Mm01220859_m1
Npy5r	Mm00443855_m1
Npy6r	Mm00627550_m1
Nr3c1	Mm00433832_m1
Nr4a1	Mm01300401_m1
Pim2	Mm00454579_m1
Pmaip1	Mm00451763_m1
Polb	Mm00448234_m1
Prf1	Mm00812512_m1
Ptger2	Mm00436051_m1
Ripk1	Mm00436354_m1
Rnf128	Mm00480990_m1
Sell	Mm00441291_m1
Sphk2	Mm00445021_m1
Stat3	Mm01219775_m1
Stat6	Mm01160477_m1
Tbp	Mm00446973_m1
Tbx21	Mm00450960_m1
Tgfb1	Mm01178820_m1
Tnfa	Mm00443258_m1
Tnfrsf10b	Mm00457866_m1
Tnfrsf14	Mm00619239_m1
Tnfrsf4	Mm00442039_m1
Tnfrsf9	Mm00441899_m1
Tnfsf10	Mm01283606_m1
Tnfsf14	Mm00444567_m1
Tnfsf8	Mm00437153_m1
Traf1	Mm00493827_m1
Traf2	Mm00801978_m1
Traf3	Mm00495752_m1
Trp53bp2	Mm00557629_m1
Xiap	Mm01311594_mH
Zbtb16	Mm01176868_m1
Zc3hc1	Mm01168068_m1